Electronic Supplementary Material (ESI) for Soft Matter.

SUPPORTING INFORMATION

A Thixotropic Supramolecular Metallogel with 2D Sheet Morphology : Iodine Sequestration and Column Based Dye Separation

Noohul Alam[†] *and Debajit Sarma**[†]

[†]Department of Chemistry, Indian Institute of Technology Patna, Bihar 801106, India

E-mail: debajit@iitp.ac.in

Experimental Details

Band Gap Measurement

The optical characterization of Mg@DEOA metallogel has been performed by the Uv-Vis spectrum, in the range of 300-800 nm(Figure S1). The optical band gap was calculated from Uv-Vis spectrum by using the following Tauc's equation

$$(\alpha \mathrm{h}v)^2 = A(\mathrm{h}v - E_g) \quad \text{Eq. (S1)}$$

Where E_g, α, $v$and$\mathrm{h}$ stands for band gap, absorption coefficient, frequency of light and Planck's constant. A is a constant, in the ideal case the value of A is considered as 1. The E_g of the Mg@DEOA metallogel were calculated by extrapolating in the linear region of the plot $\alpha \mathrm{h}v$ vs $\mathrm{h}v$ to $\alpha = 0$. The E_g was calculated to be 3.65 eV.

Adsorption Studies

To calculate adsorption capacity at equilibrium $q_e(mg/g)$,removal percentage (*R%*) at equilibrium and the amount of dye adsorbed at a particular time t, $(q_t)$the following equationswere used (Eq. S2, S3 and S4).

$$q_e = \frac{(C_0 - C_e)V}{m} \quad \text{Eq. (S2)}$$

$$R(\%) = \left[\frac{C_0 - C_t}{C_0}\right] \times 100 \quad \text{Eq. (S3)}$$

$$q_t = \frac{(C_0 - C_t)V}{m} \quad \text{Eq. (S4)}$$

Where, C_0(mg/L) stand for initial concentrations, *Ce* (mg/L) stands for equilibrium concentrations, and C_t (mg/L) represent the concentration ata particular time. *V (L)* represents the total volume of dye solution, and *m (g)*represents the adsorbent weight, respectively.

Kinetic study

To understand the adsorption behaviour of Mg@DEOAxerogel, we have performed the adsorption kinetic experiments (Figure S2). For better understanding, the linear form of the two kinetic models pseudo-first-order and pseudo-second-order were employed to examine the behaviour.

The pseudo-first-order kinetic equation is represented as

$$q_t = q_e\left(1 - e^{-k_1 t}\right) \quad \text{Eq. (S5)}$$

Where; q_t (mg/g) andq_e (mg/g) stands for the amounts of dyes adsorbed at a given time interval t (min) and dyes adsorbed at equilibrium respectively. Where k_1(min^{-1}) is the pseudo-first-order rate constant.

The pseudo-second-order adsorption rate equation is represented as

$$q_t = \frac{q_e^2 k_2 t}{1 + q_e^2 k_2 t} \quad \text{Eq. (S6)}$$

where k_2(g/mg·min) is the pseudo-second-order rate constant.

The kinetic parameters calculated with the help of pseudo-first-order and pseudo-second-order kinetic models for iodine are represented in Table S2. The value of correlation coefficient (R^2) by applying the pseudo-first-order kinetic modal is 0.8444 for iodine. However, R^2 values by applying the pseudo-second-order models for iodine are 0.9172. The obtained results from

both models are clearly indicating that the pseudo-second-order model seems best fitted. Furthermore, the $q_{e,cal}$ (calculated) values are much closer to $q_{e,exp}$ (experimental) values by applying the pseudo-second-order model in comparison to the pseudo-first-order model (Table S2). From these results, we can say that the adsorption process of iodine on Mg@DEOA xerogel follow the pseudo-second-order model.

Adsorption Isotherm

To understand the adsorption process of Mg@DEOA material, adsorption isotherms were taken into account as it provides information about the distribution of adsorbate between the solid and liquid phases. Herein,three different adsorption modelsLangmuir, FreundlichandLangmuir-Freundlich adsorption isothermwere used. The Langmuir model talks about the adsorption on homogeneous surface, and this model is based on three basic assumptions that, all the adsorption sites are identical and each site is able to take only one molecule, the adsorption energy is constant, and it is independent of surface coverage, and after adsorption adsorbate molecule cannot exchange their site to another (Eq. S7).[1]The Freundlich adsorption isotherm model talks about the multilayer adsorption on the energetically heterogeneous surface (Eq.S8).[2] However, the Langmuir-Freundlich adsorption isotherm model is the extension of Langmuir and Freundlich model,which reduces to the Langmuir model at high surface coverage, and to Freundlich model for low surface coverage (Eq. S9).[1, 3]

Langmuir isotherm model

$$Q_e = \frac{Q_{max} K_L C_e}{1 + K_L C_e} \quad \text{Eq. (S7)}$$

Freundlich isotherm model

$$Q_e = K_F C_e^{1/n_F} \quad \text{Eq. (S8)}$$

Langmuir-Freundlichisotherm model

$$Q_e = \frac{Q_{max}(K_g C_e)^{1/n_{LF}}}{1 + (K_g C_e)^{1/n_{LF}}} \quad \text{Eq. (S9)}$$

Recyclability test

Recyclability of the iodine capture by Mg@DEOA xerogel was studied (Figure S10), using the xerogel collected by centrifugation after each cycle and then immersing in the fresh ethanol for 2 hours. Followed by washing with diethyl ether then the adsorbent kept for drying under vacuum, for reusing in the next cycle. The adsorption-desorption cycle was carried out for four times, the obtained result suggested that Mg@DEOA xerogel could be utilized up to four cycles with removal efficiency of 53 %. However, for the dyes, we were unable to perform the recyclability test because the adsorbent was not degenerating for the second cycle after immersing the dye loaded xerogel in the ethanol, diethyl ether, and even after addition of NaOH/HCl.

Dyes and iodine adsorption by Mg@DEOA-gel

We have performed dye and iodine adsorption experiment to understand the behaviour of Mg@DEOA in the gel state (Mg@DEOA-gel). 4 ml of each CR (50 mg/L), MO (50 mg/L) dyes and 2 ml of iodine (500 mg/L) were poured in the Mg@DEOA-gel containing vials. After 6 hours, the Uv-vis adsorption analysis was performed to understand the adsorption behaviour of Mg@DEOA-gel. The comparison of UV−vis data of dye samples before and after the adsorption shows 65% and 57% removal efficiency for the CR and MO dyes respectively. Similarly, for iodine, 40% removal efficiency was observed. The result revealed that the gel material exhibit less removal efficiency as compared to the dried form of Mg@DEOA material (xerogel). It may be because of the Mg@DEOA-gel contain a large amount of solvent molecule in their gel matrix, however, Mg@DEOA-xerogel matrix is free of solvent molecules, i.e. material pores are free. Therefore, xerogel can interact more profoundly than gel form of the material.

Leaching test of iodine from iodine loaded xerogel

We have monitored the leaching behaviour of iodine loaded sample after immerging in the fresh hexane solution. Initially, 30 mg of iodine loaded xerogel was kept in the glass vial then 2 ml fresh hexane solution was poured. By necked eye, we did not observe any colour change of fresh hexane solution containing iodine loaded sample. After 6 hours, we have performed the Uv-vis spectroscopy analysis of the solution. Uv-vis adsorption spectrum (Figure S12), clearly shows that iodine the leaching of iodine is negligible in the fresh hexane solution. However, after adding∽2 ml of ethanol in the same solution (fresh hexane solution with iodine loaded xerogel), within few minutes the colour of the solution turned light yellowish from colourless. The obtained result suggests that Mg@DEOA material is a stable host matrix to capture iodine from the hexane.

Figure Caption

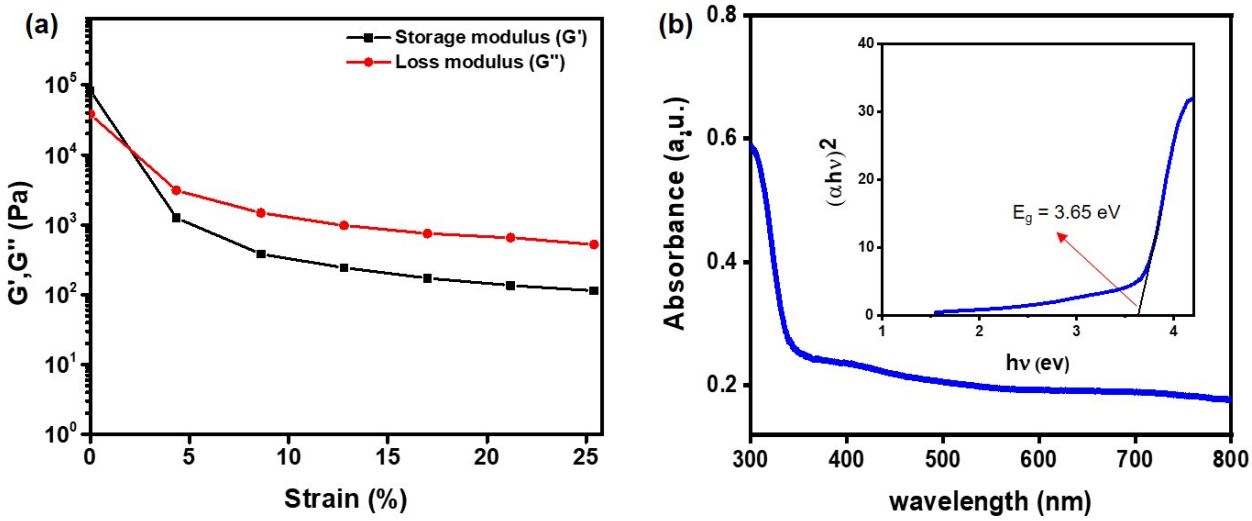

Figure S1. Strain-sweep measurements, (b) UV−vis absorption spectra and Tuac's plots (inset) for Mg@DEOA.

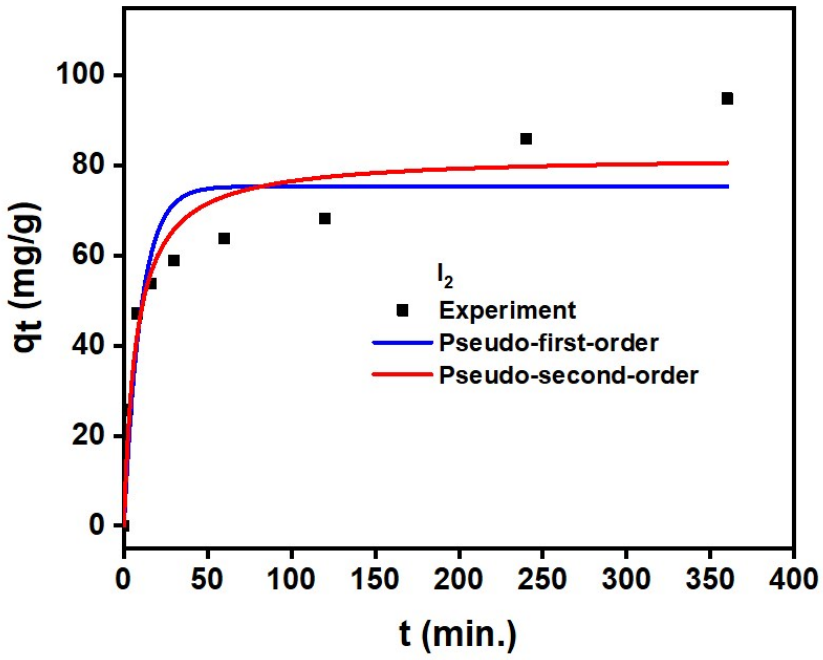

Figure S2. Data fitted in the pseudo-first-order kinetic model and the pseudo-second-order kinetic model (iodine 500 mg/L) of the Mg@DEOA.

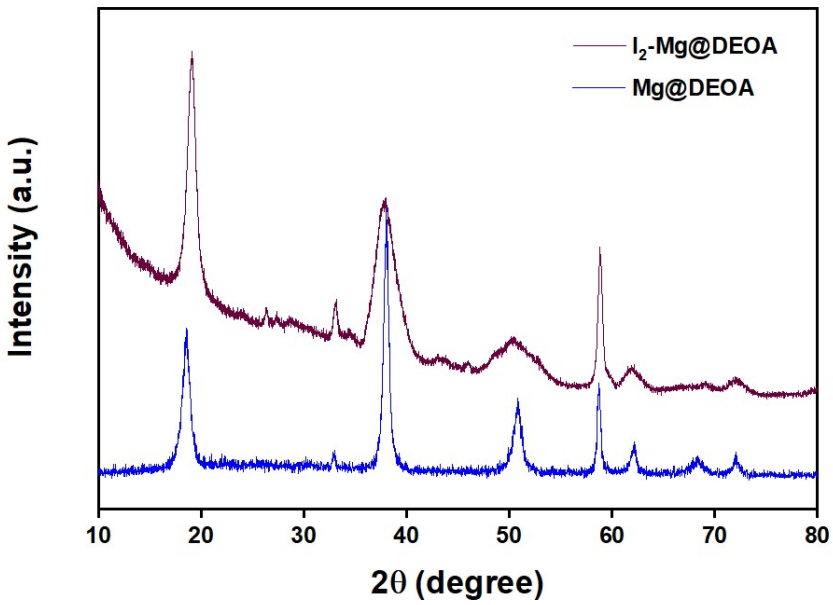

Figure S3. Powder X-ray diffraction pattern of Mg@DEOA xerogel before and after iodine sorption.

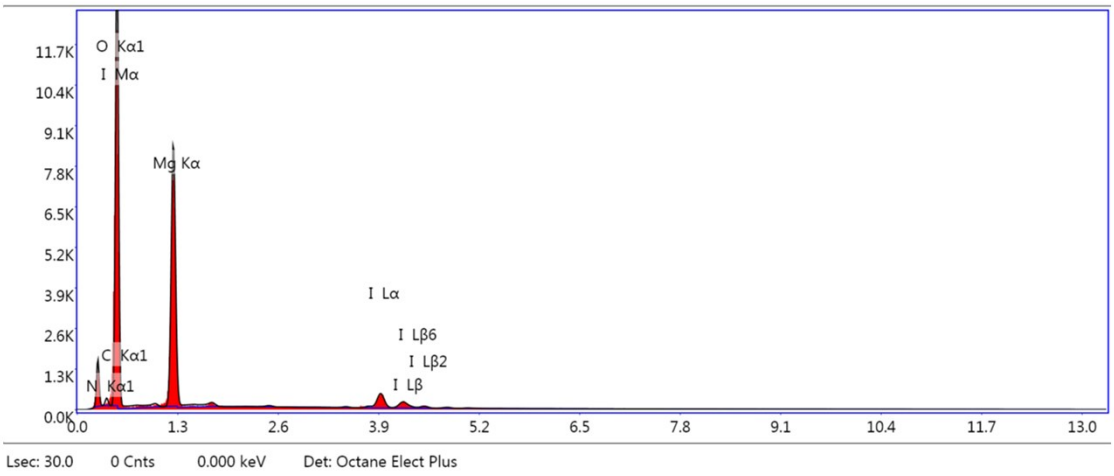

Figure S4. EDS image of Mg@DEOA xerogels after desorption of iodine in ethanol.

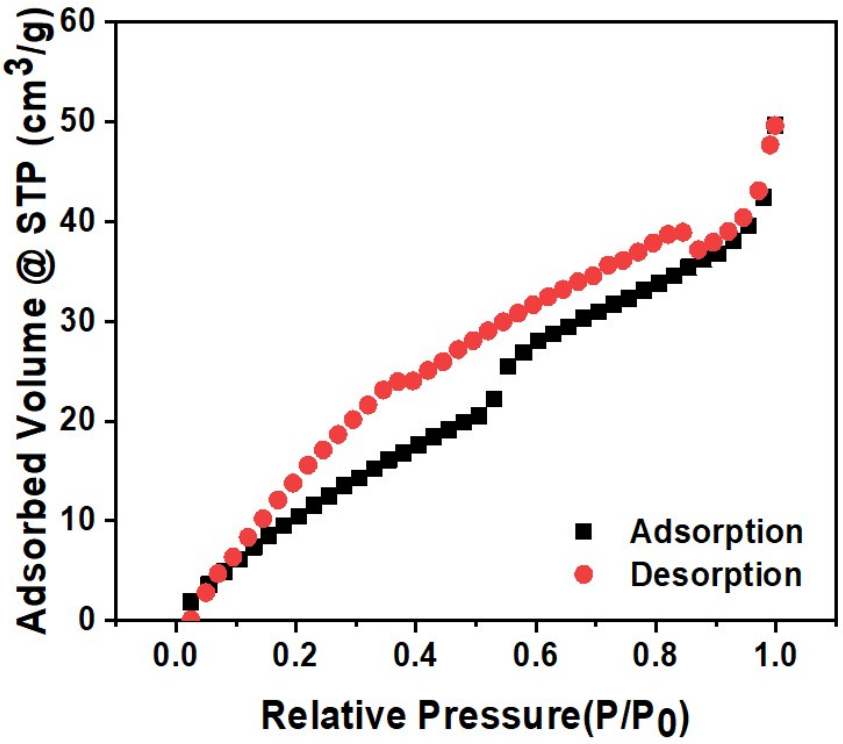

Figure S5. N2 sorption isotherm Mg@DEOA xerogels after desorption of iodine in ethanol.

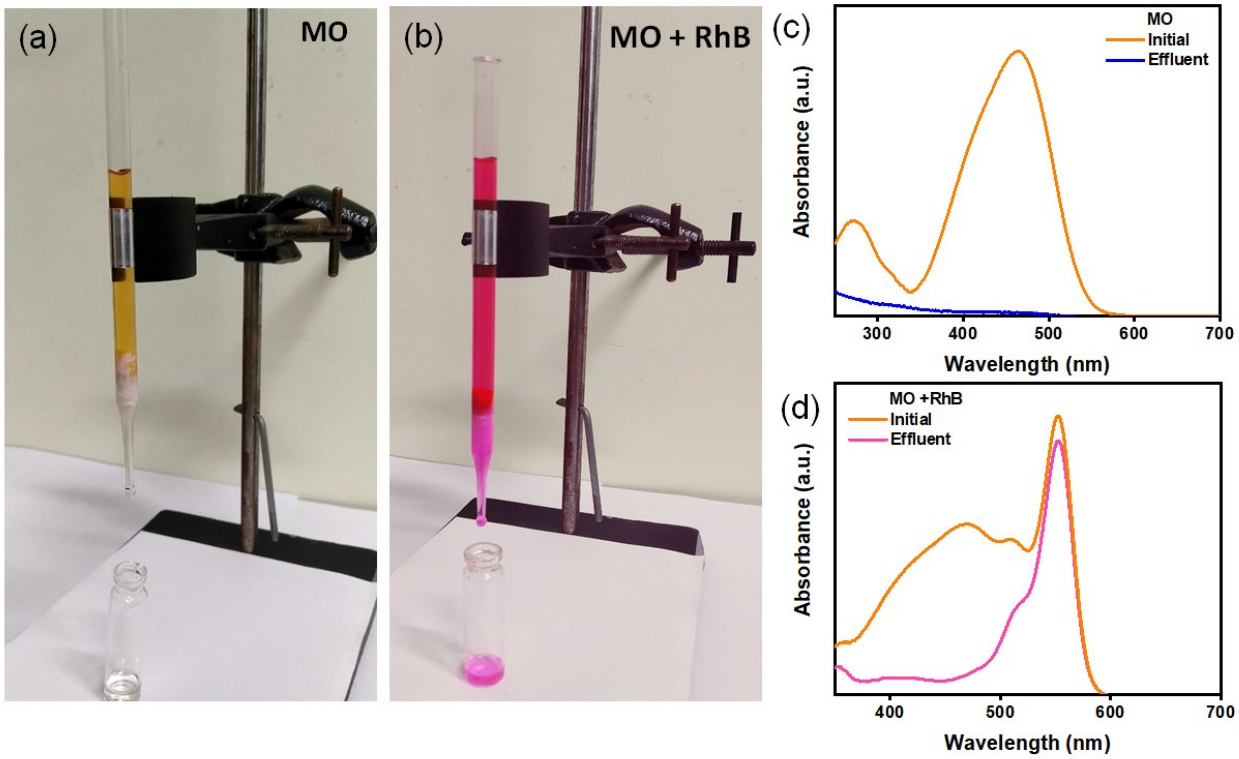

Figure S6. (a) Removal MO dye from water, (b) separation of RhB dye from the mixture of MO/RhB dyes; uv-vis spectra before and after (c) removal of MO dye, and (d) separation of MO dye from the mixture MO/RhB dyes.

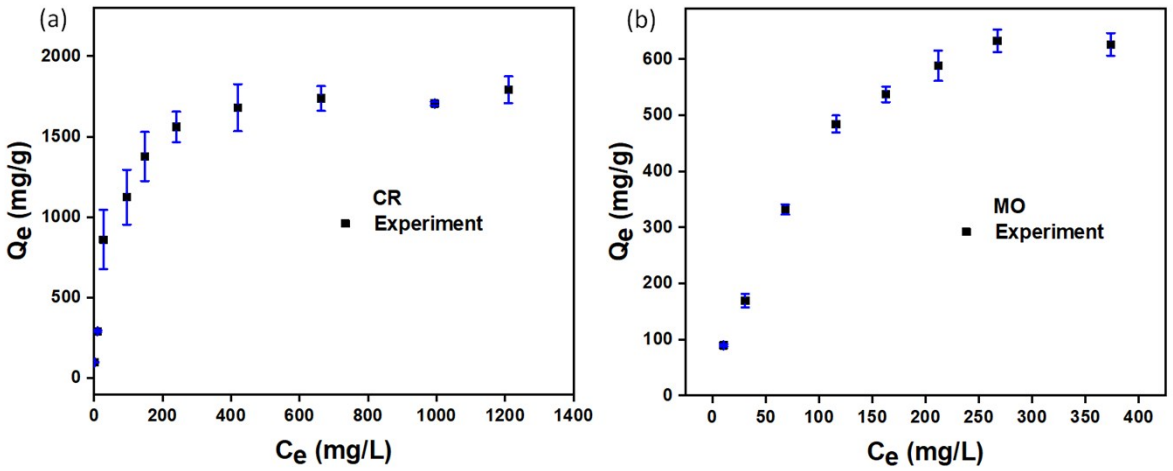

Figure S7. Adsorption isotherms for (a) CR and (b) MO on Mg@DEOA.

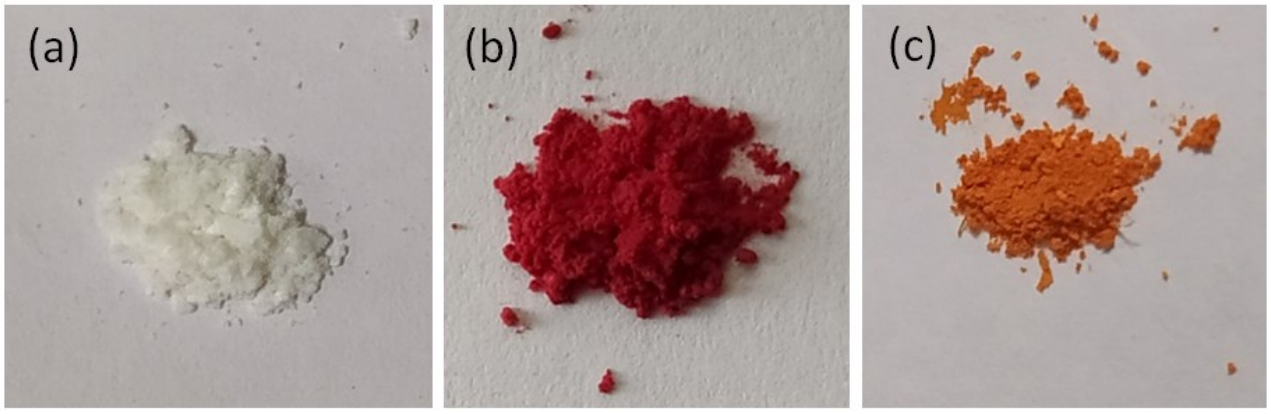

Figure S8. Images of Mg@DEOA xerogel (a) before, and after (b) CR and (c) MO dye adsorption.

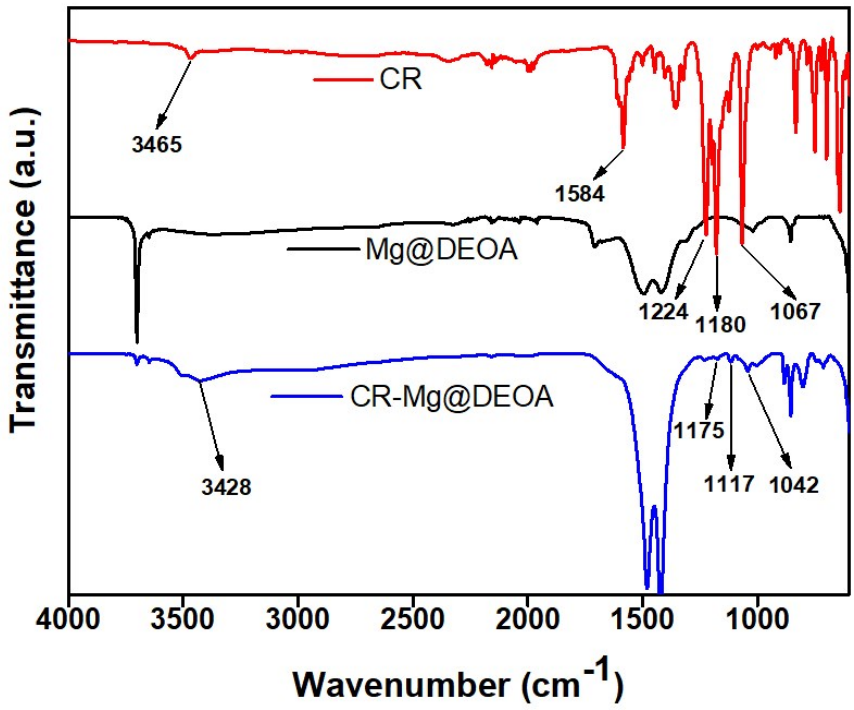

Figure S9. IR spectrum of congo red, Mg@DEOA xerogel and congo red adsorbed Mg@DEOA xerogel.

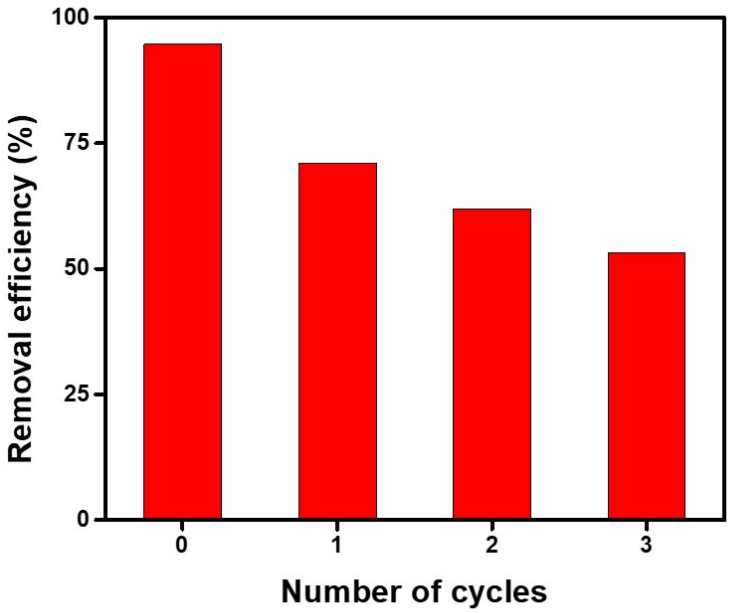

Figure S10. Recyclability test of Mg@DEOA xerogel for iodine adsorption from hexane solution at initial concentration of 500 mg/L.

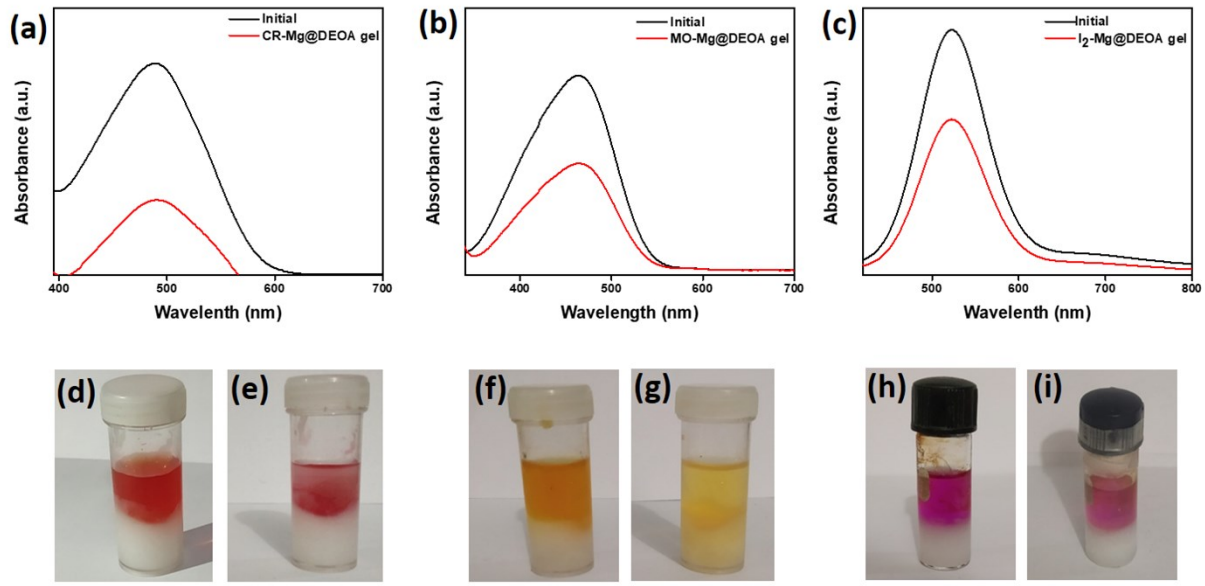

Figure S11. Uv-vis spectra of removal of (A) CR dye, (b) MO dye from water and (c) iodine from hexane by Mg@DEOA gel. Removal of dyes from water by Mg@DEAO gel (d) image after addition of CR dye and (e) after 6 h, (f) image after addition of MO dye and (g) after 6 h. Removal of iodine from hexane (h) image after addition of iodine solution and (d) after 6 h.

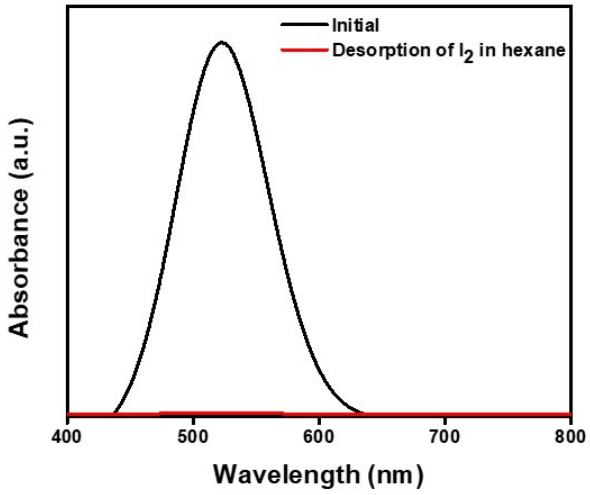

Figure S12. Desorption test of iodine from the iodine loaded xerogel after immersing in fresh hexane solution.

TableS1. Comparison of the surface area of Mg@DEOA metallogel with reported metallogels.

Sr. No.	Metallogel	Surface area ($m^2 g^{-1}$)	References
1	MOG [Cu- 2,6-bis(2-benzimidazolyl) pyridine]-xerogel	9.75	4
2	MOG-1 [Cd-Na_2HL]-xerogel	31.86	5
3	Al-PDC [Aluminium-pyridine dicarboxylic acid]-xerogel	40.68	6
4	CPG1-xerogel	223	7
5	CuA-Ox xerogel	67	8
6	poly[methyl vinyl ether-alt-mono-sodium maleate]-AgNO3, xerogel	70	9
7	$Zn_{0.90}Co_{0.10}$-BMOG-xerogel	92.5	10
8	copper triflate xerogel	106.9	11
9	FNPA xerogel	124	12
10	**Mg@DEAO-xerogel**	**180.77**	**This work**

Table S2. Adsorption kinetic parameters of iodine with Mg@DEOA.

Model	**Parameters**	**Iodine**
	$q_{e,exp}$ (mg/g)	94.83
Pseudo-first-order	$q_{e,cal}$ (mg/g)	75.33
	K_1	0.0991
	R^2	0.8444
Pseudo-second-order	$q_{e,cal}$ (mg/g)	82.22
	K_2	0.0016
	R^2	0.9172

Table S3. Langmuir, Freundlich and Langmuir-Freundlich models isotherm parameters for iodine, congo red (CR), and methyl orange (MO).

Models	**Langmuir**			**Freundlich**			**Langmuir-Freundlich**			
Parameters	Q_{max}	k_L	R^2	n_F	k_F	R^2	Q_{max}	n_{LF}	K_g	R^2
Iodine	586.63	0.0026	0.9635	0.41	24.97	0.9519	715.92	1.30	0.0016	0.9675
CR	1812.85	0.0239	0.9852	0.24	339.91	0.8851	1868.11	1.12	0.2219	0.9867
MO	833.30	0.0105	0.9841	0.44	2.24	0.9296	731.98	0.78	0.1366	0.9911

Table S4. Comparison of adsorption capacity of our synthesized materials with different reported adsorbents.

Sr. No.	Adsorbent	Iodine/Dye/CO_2	Adsorption capacity (mg/g)	References
1	FCMP-600@1	I_2	550	13
2	[Cd(ABTC)(H_2O)$_2$(DMA)].4DMA	I_2	680	14
3	JLUE-SOF-3-DMSO	I_2	207	15
4	1-SDS@P5A-POM	I_2	190	16
5	5-SDS@P5A-POM	I_2	360	16
6	ZnO (CZ-400)	Congo red	500	17
7	Fe_3O_4@ZTB-1	Congo red	458	18
8	$MgFe_2O_4$-OH NPs	Congo red	67	19
9	Tetraphenylethene-linked nanoporous polymers	Congo red	1040	20
10	Ni/Mg/Al layered double hydroxides	Congo red	1250	21
11	Graphene oxide-chitosan/silica	Congo red	294	22
12	Ni@MG1 xerogel	Congo red	1428	23
13	F-PANI2 xerogel at pH7	Methyl orange	148	24
14	BMG-3 xerogel	Methyl orange	40	25
12	AgBr-AgBr/CTAB nanomaterials	Methyl orange	104	26
13	Cu_2O−Ag	Methyl orange	976	27
14	PANI- Co_3O_4 Nanocomposite	Methyl orange	107	28
15	**Mg@DEOA**	**I_2** **Congo red** **Methyl orange**	**586** **1812** **833**	**This work**

Table S5. The dye removal efficiency of Mg@DEOA for CR, MO dyes, and mixture of dyes CR/RhB and MO/ RhB dyes.

Sr. no.	Dye	Effluent colour	Removal efficiency (%)	% of RhB separation from a mixture of dyes
1.	CR	Colourless	99.04	-
2.	MO	Colourless	98.82	-
3.	CR + RhB	Magenta (RhB colour)	-	85.45
4.	MO +RhB	Magenta (RhB colour)	-	91.07

REFERENCES

1. D. Sarma, C. D. Malliakas, K. Subrahmanyam, S. M. Islam and M. G. Kanatzidis, *Chem. Sci.*, 2016, **7**, 1121-1132.
2. X. Wang, C. Zhan, Y. Ding, B. Ding, Y. Xu, S. Liu and H. Dong, *ACS Sustain. Chem. Eng.*, 2017, **5**, 1457-1467.
3. S. Azizian, S. Eris and L. D. Wilson, *Chem. Phys.*, 2018, **513**, 99-104.
4. Z. W. Peng, D. Yuan, Z. W. Jiang and Y. F. Li, *Electrochim. Acta.*, 2017, **238**, 1-8.
5. C. K. Karan and M. Bhattacharjee, *ACS Appl. Mater. Interfaces*, 2016, **8**, 5526-5535.
6. S. Bhowal, A. Ghosh, S. P. Chowdhuri, R. Mondal and B. B. Das, *Dalton. Trans.*, 2018, **47**, 6557-6569.
7. R. D. Mukhopadhyay, V. K. Praveen, A. Hazra, T. K. Maji and A. Ajayaghosh, *Chem. Sci.*, 2015, **6**, 6583-6591.
8. S. Saha, E. M. Schön, C. Cativiela, D. Diaz Diaz and R. Banerjee, *Chem.: Eur. J.*, 2013, **19**, 9562-9568.
9. F. Xu, H. Padhy, M. Al-Dossary, G. Zhang, A. R. Behzad, U. Stingl and A. Rothenberger, *J. Mater. Chem. B*, 2014, **2**, 6406-6411.
10. H. Guo, Q. Feng, K. Xu, J. Xu, J. Zhu, C. Zhang and T. Liu, *Adv. Funct. Mater.,* 2019, **29**, 1903660.
11. S. Sengupta and R. Mondal, *RSC Adv.*, 2016, **6**, 14009-14015.
12. H. B. Aiyappa, S. Saha, P. Wadge, R. Banerjee and S. Kurungot, *Chem. Sci.*, 2015, **6**, 603-607.
13. G. Li, C. Yao, J. Wang and Y. Xu, *Sci. Rep.,* 2017, **7**, 1-8.
14. C. Yao, W. Wang, S.-R. Zhang, H.-Y. Li, Y.-H. Xu, Z.-M. Su and G.-B. Che, *RSC Adv.*, 2018, **8**, 36400-36406.

15. Y. Li, H. Yu, F. Xu, Q. Guo, Z. Xie and Z. Sun, *CrystEngComm*, 2019, **21**, 1742-1749.

16. M. Zeng, J. Tan, K. Chen, D. Zang, Y. Yang, J. Zhang and Y. Wei, *ACS Appl. Mater. Interfaces*, 2019, **11**, 8537-8544.

17. S. Lan, L. Liu, R. Li, Z. Leng and S. Gan, *Ind. Eng. Chem. Res.*, 2014, **53**, 3131-3139.

18. L.-J. Han, F.-Y. Ge, G.-H. Sun, X.-J. Gao and H.-G. Zheng, *Dalton. Trans.*, 2019, **48**, 4650-4656.

19. C. Aoopngan, J. Nonkumwong, S. Phumying, W. Promjantuek, S. Maensiri, P. Noisa, S. Pinitsoontorn, S. Ananta and L. Srisombat, *ACS Appl. Nano Mater.*, 2019, **2**, 5329-5341.

20. H. Liu and H. Liu, *J. Mater. Chem. A*, 2017, **5**, 9156-9162.

21. C. Lei, X. Zhu, B. Zhu, C. Jiang, Y. Le and J. Yu, *Hazard. Mater.*, 2017, **321**, 801-811.

22. Q. Du, J. Sun, Y. Li, X. Yang, X. Wang, Z. Wang and L. Xia, *Chem. Eng. J.*, 2014, **245**, 99-106.

23. N. Alam and D. Sarma, *ACS Omega*, 2020, **5**, 17356-17366.

24. S. Das, P. Chakraborty, R. Ghosh, S. Paul, S. Mondal, A. Panja and A. K. Nandi, *ACS Sustain. Chem. Eng.*, 2017, **5**, 9325-9337.

25. K. Sarmah, G. Pandit, A. B. Das, B. Sarma and S. Pratihar, *Cryst. Growth Des.*, 2017, **17**, 368-380.

26. L. Tang, J.-j. Wang, L. Wang, C.-t. Jia, G.-x. Lv, N. Liu and M.-h. Wu, *ACS Sustain. Chem. Eng.*, 2016, **4**, 4617-4625.

27. A. K. Sasmal, J. Pal, R. Sahoo, P. Kartikeya, S. Dutta and T. Pal, *J. Phys. Chem. C*, 2016, **120**, 21580-21588.

28. S. Shahabuddin, N. M. Sarih, S. Mohamad and S. N. A. Baharin, *RSC Adv.*, 2016, **6**, 43388-43400.